Charge carrier density dependence of the hole mobility in poly(p-phenylene vinylene)

Tanase, C; Blom, PWM; de Leeuw, DM; Meijer, EJ

Published in:
Physica Status Solidi A-Applied Research

DOI:
10.1002/pssa.200404340

Publication date:
2004

phys. stat. sol. (a) **201**, No. 6, 1236–1245 (2004) / **DOI** 10.1002/pssa.200404340

Charge carrier density dependence of the hole mobility in poly(*p*-phenylene vinylene)

C. Tanase[1], **P. W. M. Blom**[*, 1], **D. M. de Leeuw**[2], and **E. J. Meijer**[2]

[1] Materials Science Centre, University of Groningen, Nijenborgh 4, 9747 AG Groningen, The Netherlands
[2] Philips Research Laboratories, 5656 AA Eindhoven, The Netherlands

Received 30 January 2004, revised 23 March 2004, accepted 29 March 2004
Published online 6 May 2004

PACS 71.20.Rv, 72.80.Le, 73.61.Ph

The hole transport in various poly(*p*-phenylene vinylene) (PPV) derivatives has been investigated in field-effect transistors (FETs) and light-emitting diodes (LEDs) as a function of temperature and applied bias. The discrepancy between the experimental hole mobilities extracted from FETs and LEDs based on a single disordered polymeric semiconductor originates from the strong dependence of the hole mobility on the charge carrier density. The microscopic charge transport parameters are directly related to the chemical composition of the analysed polymers. By chemically modifying the PPV, the hole mobility in both FETs and LEDs can be changed by orders of magnitude. For highly disordered PPVs it is demonstrated that the exponential density of states (DOS), which is used to describe the charge transport in FETs, is a good approximation of the tail states of the Gaussian DOS, which describes the charge transport in LEDs. Increase of the directional order in the PPV film enhances the mobility but also induces a strong anisotropy in the charge transport, thereby obscuring a direct comparison between sandwich and field-effect devices.

1 Introduction

Solution-processable conjugated polymers have attracted attention because of their potential advantages in developing low-cost microelectronic devices such as light-emitting diodes (LEDs) [1, 2] and field-effect transistors (FETs) [3, 4]. An important factor in understanding and developing the devices based on organic semiconductors is the mechanism of charge carrier transport. It has become clear that the charge transport in these devices is dominated by structural and energetic disorder both in LEDs [5, 6] and FETs [7, 8].

Poly(*p*-phenylene vinylene) (PPV) is considered a suitable semiconductor for LEDs, being extensively studied in the last decade due to its high photoluminescence yields and high values of the hole mobility [9]. The charge transport in PPV is described by a theoretical model based on thermally assisted intermolecular hopping of charges in a correlated Gaussian disordered system [6]. The Gaussian density of states (DOS) reflects the energetic spread of the charge transport sites. This energetic spread is the result of the fluctuation in the local conjugation length and structural disorder.

Field-effect transistors have shown great improvements during the last years. Reference [10] gives an overview of the scientific and technological knowledge of organic thin-films transistors. Recently, flexible active-matrix monochrome electrophoretic displays based on solution processed organic transistors on polyimide substrates have been demonstrated [11]. The charge transport in p-type disordered organic FETs is described by variable range hopping of localised charges in an exponential DOS [12]. It has been

* Corresponding author: e-mail: P.W.M.Blom@phys.rug.nl

recently demonstrated that the charge carrier mobility and the charge transport properties are dependent on the charge carrier density [12–14].

The focus in this review is on the charge transport in the conjugated polymer PPV and its derivatives studied as the active layer in LEDs and FETs. Chemical modification of PPV provides a tool to control the backbone and side chains of the polymer and influences both the electronic and morphologic properties. Different side chains attached to the polymer result in different structural configurations and hence the conductive properties of the polymer can be modified. Therefore, the molecular structure of the polymer chains can strongly affect the charge carrier mobility. Theoretically, the hole transport in LEDs is described differently than in FETs. We study the dependence of the hole mobility in PPV derivatives with different side chains and correlate the hole mobility obtained from diodes with the hole mobilities obtained from field-effect transistors.

For a single PPV, the hole mobility determined from LEDs shows big differences with the hole mobility determined from FETs, up to 3 orders of magnitude [13]. The large mobility differences obtained from the two types of devices originate from the strong charge carrier dependence of the mobility [13]. The mobility description at low charge carrier density (in a LED) using a Gaussian DOS is correlated to the mobility description at high charge carrier density (in a FET) using an exponential DOS. The only difference in this case is the energy position and energy range over which the Fermi level moves in the DOS, in the operational regime of the two devices. The temperature and charge carrier dependence of the hole mobility are unified in a single charge transport model for disordered PPV derivatives. In more ordered PPVs the charge transport is observed to be anisotropic with respect to the in-plane (FET) and out-of-plane (LED) transport and cannot be unified.

2 Experimental results and discussion

In the present study we focus on three PPV-derivatives, which are used as active layers in LEDs and FETs. The materials are poly(2-methoxy-5-(3′,7′-dimethyloctyloxy)-*p*-phenylene vinylene) (OC_1C_{10}-PPV), poly[2,5-bis(3′,7′-dimethyloctyloxy)-*p*-phenylene vinylene] ($OC_{10}C_{10}$-PPV) and a random copolymer of poly(2-methoxy-5-(3′,7′-dimethyloctyloxy)-*p*-phenylene vinylene) and poly[4′-(3,7-dimethyloctyloxy)-1,1′-biphenylene-2,5-vinylene] (NRS-PPV). The chemical structures corresponding to these PPV-derivatives are presented in Fig. 1. In all devices the polymer has been spin-coated from a toluene solution.

2.1 Charge carrier mobility in hole-only diodes

The schematic structure of the hole-only diode used in the experiments is presented in the inset of Fig. 2. Figure 2 displays a typical example of the temperature dependent current density-voltage characteristics

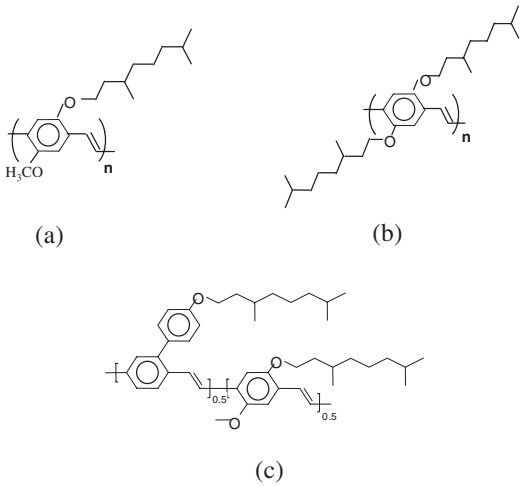

Fig. 1 Chemical structures of OC_1C_{10}-PPV (a), $OC_{10}C_{10}$-PPV (b) and NRS-PPV (c).

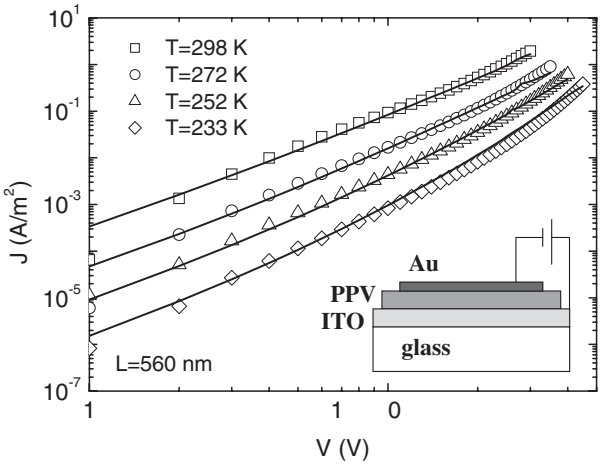

Fig. 2 Temperature dependent current-density vs. voltage characteristics of NRS-PPV hole-only diode. The solid lines represent the prediction from the SCL model including the field dependent mobility.

($J-V$) of a PPV hole only device (NRS-PPV). The current density through PPVs contacted with ITO is space-charge limited (SCL) and shows a strong dependence on both the temperature, T, and the applied electric field, E [15]. At low bias voltages the hole mobility is constant, whereas at high bias voltages the dependence of the mobility on the voltage has to be taken into account. The increase of μ_{LED} with electric field reflects the lowering of the hopping barriers in the direction of the applied electric field, which exponentially enhances the hopping probability. The charge transport in disordered organic semiconductors proceeds by means of hopping in a Gaussian site-energy ε distribution:

$$\mathrm{DOS}_{\mathrm{Gauss}} = \frac{N_t}{\sqrt{2\pi}\,\sigma} \exp\left(-\frac{\varepsilon}{2\sigma^2}\right), \tag{1}$$

where N_t is the number of states per unit volume and σ is the width of the Gaussian [5]. It has been demonstrated that the hole mobility in PPV derivatives is well described by a 3-D transport model based on hopping in a correlated Gaussian disordered model [6]:

$$\mu_{\mathrm{LED}} = \mu_0 \exp\left[-\left(\frac{3\sigma}{5k_BT}\right)^2 + 0.78\left(\left(\frac{\sigma}{k_BT}\right)^{1.5} - \Gamma\right)\sqrt{\frac{eEa}{\sigma}}\right], \tag{2}$$

where μ_0 is the zero-field mobility in the limit $T \to \infty$, σ the width of the Gaussian density of states (DOS), Γ gives the geometrical disorder, and a the average intersite spacing. The lines in Fig. 2 represent the prediction of SCL model with field dependent mobility given by Eq. (2) using $\Gamma = 6$ and $a = 1.1$ nm and are in excellent agreement with the experimental data. Similar study has been done for OC_1C_{10}-PPV and $OC_{10}C_{10}$-PPV [16]. The hole mobility for low electric fields at room temperature for the polymers studied in this paper are presented in Table 1. The zero-field mobility for all three polymers is plotted in Fig. 3 as function of T^{-2}. Modelling the mobility data with $\ln(\mu_{\mathrm{LED}}(E=0)) \approx T^{-2}$ the width of the Gaussian DOS is determined and the values of σ for the PPV-derivatives are presented in Table 1. Within the

Table 1 Parameters $\mu_{\mathrm{LED}}(E=0)$ (zero-field mobility) at room temperature and σ (the width of the Gaussian density of states) for the PPV-derivatives as determined from hole-only diode.

polymer	$\mu_{\mathrm{LED}}(E=0)$ ($\mathrm{m^2/Vs}$)	σ (meV)
$OC_{10}C_{10}$-PPV	9.0×10^{-10}	93
OC_1C_{10}-PPV	5.0×10^{-11}	110
NRS-PPV	1.5×10^{-12}	125

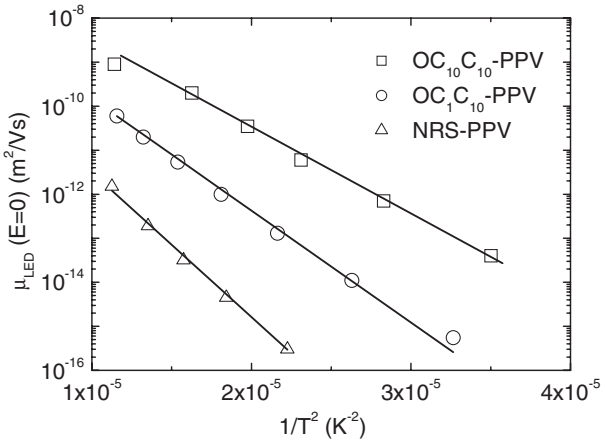

Fig. 3 Temperature dependence of the zero-field mobility $\mu_{LED}(E = 0)$ for NRS-PPV, OC_1C_{10}-PPV and $OC_{10}C_{10}$-PPV hole-only diode.

temperature range studied, the zero-field mobility of the samples examined is in good agreement with the predictions of the correlated Gaussian disorder model (solid lines in Fig. 3). From Fig. 3 we find that chemical modification of PPV can result in a change in the zero-field mobility by orders of magnitude. Furthermore, the magnitude of the mobility is correlated to the amount of energetic disorder. For stronger disorder the energy barriers which the charge carriers have to jump become higher, leading to a lower mobility. The lowest value for σ is obtained for $OC_{10}C_{10}$-PPV. Compared to OC_1C_{10}-PPV, which has two asymmetric side chains, $OC_{10}C_{10}$-PPV has two long symmetric OC_{10} side chains which cancel any effect of the interaction between side chains on the conformation. From studies of the morphology of these two polymer films with phase-imaging scanning force microscopy it has been demonstrated that the symmetry of substitution is related to surface morphology and aggregation behaviour [17]. $OC_{10}C_{10}$-PPV shows straight, aligned individuals chains and strong aggregation, while spiralling chains and no aggregation were observed for the asymmetrical OC_1C_{10}-PPV. In comparison with $OC_{10}C_{10}$-PPV, the configurationally freedom of OC_1C_{10}-PPV will result in a larger energetic spread between the electronic levels of individual chain segments and therefore a larger σ for the Gaussian DOS. NRS-PPV is a random copolymer, which means from the aggregation point of view a much stronger structural disorder than the other two polymers and as a consequence it has a larger σ.

2.2 Local mobility versus field-effect mobility in FETs

The schematic structure of the p-type field-effect transistor used in the experiments is presented in the inset of Fig. 4. A negative voltage applied at the gate electrode (G) of the p-type FET forces the top of the valence band to bend upwards closer to the Fermi level and induces an accumulation of holes at the semiconductor/insulator interface [18]. A small voltage V_d applied between the source (S) and the drain (D) electrodes gives rise to a source-drain current I_{ds}.

Figures 4 and 5 display typical examples for the temperature-dependent transfer characteristics of FETs based on NRS-PPV and $OC_{10}C_{10}$-PPV, respectively. The transfer characteristics have been measured in dark and in vacuum, in the linear operating regime of the transistor, by using a drain voltage $V_d = -0.1$ V, which is much smaller than the applied gate voltage ($V_g = -1$ to -20 V). The conductive channel has a width, W, of 2500 μm and a length, L, of 10 μm. The electric field in the active channel is small, such that any field dependence of the field-effect mobility in the source-drain direction can be ignored. The typical thickness of the polymer spin-coated on top of the gold source and drain contacts is 200 nm. The insulator capacitance per unit area, C_i, is 17 nF/cm^2. From the transfer characteristics the experimental field-effect mobility is determined using the following equation [19]:

$$\mu_{\mathrm{FET}}(V_g) = \frac{\partial I_{ds}}{\partial V_g} \frac{L}{WC_i V_d} . \tag{3}$$

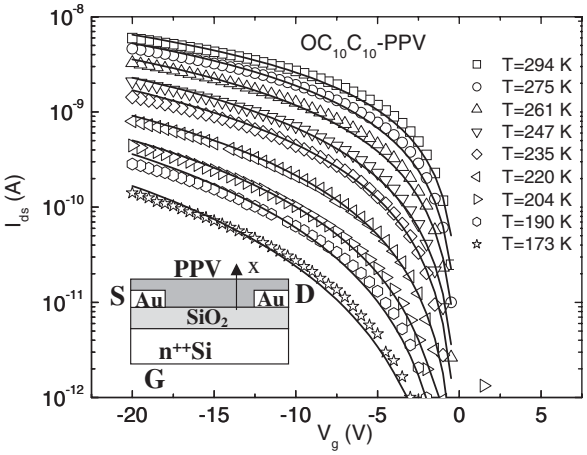

Fig. 4 Transfer characteristics of $OC_{10}C_{10}$-PPV field-effect transistor. The solid lines indicate the calculated source-drain currents. The inset shows a schematic view of an organic field-effect transistor.

In Fig. 6 the experimental field-effect mobility, μ_{FET}, is presented as determined from Eq. (3) for OC_1C_{10}-PPV for different temperatures as function of gate voltage, V_g. By using Eq. (3) we assume that all the charge carriers in the accumulation layer have the same mobility.

In disordered organic semiconductors, where the charge carriers are strongly localised, the charge transport is described by a variable range hopping model [12, 18], in contrast to conventional monocrystalline silicon. By increasing the gate voltage the induced charge carrier density in the accumulation channel increases, the lower states of the organic semiconductor are filled and any additional charges in the system will need less activation energy for the jumps to neighbouring sites. As a result the charge carrier mobility will be enhanced. In this way the dependence of the mobility on the gate bias is due to the dependence of the mobility on the charge carrier density. For the understanding of the transfer characteristics of organic semiconductors it is important to realise that in a FET the charge carrier density is not uniformly distributed in the accumulation channel in the direction perpendicular to the semiconductor/insulator interface, but depends on the distance from the interface. Therefore, the mobility that is charge carrier dependent also depends on the position in the accumulation layer. The consequence is that for a given V_g a distribution of charge carrier mobilities is present in the organic FET.

The question that arises is how the distribution of the local mobility of the charge carriers in the accumulation channel compares to the field-effect mobility as calculated from Eq. (3) for a certain gate voltage. In order to answer this question the distribution of the charge carrier density in the accumulation channel has to be calculated. An unintentionally doped system is considered. The energy levels, which

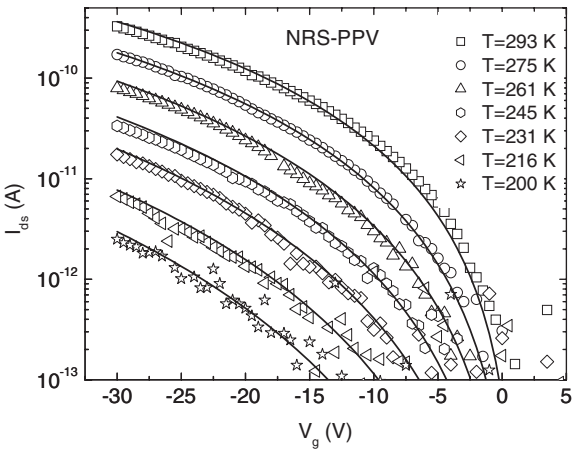

Fig. 5 Transfer characteristics of NRS-PPV field-effect transistor. The solid lines indicate the calculated source-drain currents.

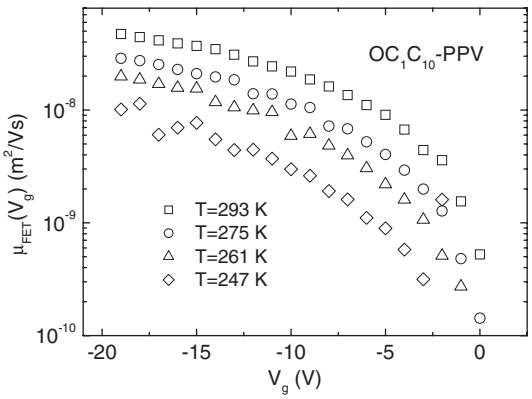

Fig. 6 Temperature dependence of the OC_1C_{10}-PPV filed-effect mobility as a function of gate voltage as determined from Eq. (3) (symbols).

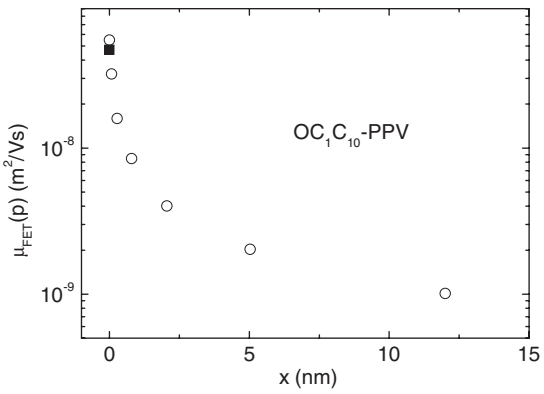

Fig. 7 Distribution of local mobility in the accumulation channel as a function of the distance from the semiconductor/insulator interface of an undoped semiconductor for $V_g = -19$ V.

are responsible for charge transport, are characterized by an exponential density of states:

$$\mathrm{DOS}_{\mathrm{exp\,on}} = \frac{N_t}{k_B T_0} \exp\left(\frac{\varepsilon}{k_B T_0}\right) \tag{4}$$

where k_B is Boltzmann's constant, T_0 indicates the width of the exponential distribution. The total concentrations of charges in the semiconductor layer are given by the formula:

$$p = \int_{\varepsilon} \mathrm{DOS}_p(\varepsilon)\, f_p(\varepsilon)\, \mathrm{d}\varepsilon \tag{5}$$

$$n = \int_{\varepsilon} \mathrm{DOS}_n(\varepsilon)\, f_n(\varepsilon)\, \mathrm{d}\varepsilon \tag{6}$$

where p, n represent the density of majority and minority charge carriers, $f_p(\varepsilon)$, $f_n(\varepsilon)$ represent the Fermi-Dirac distribution function for holes and electrons. The position of the Fermi level can be found from the preservation of the electrical charges $n + N_A^- = p$, where N_A^- is the number of ionized acceptors. By applying a negative voltage the equilibrium between the charges in the semiconductor is changed due to the local internal potential or band bending $V(x)$, where the x direction is perpendicular to the semiconductor/insulator interface. In this situation the Fermi level becomes $E_f(x) = E_f - qV(x)$. Combining this with Eqs. (5, 6) then provides the relation between the charge concentration (p, n) and the potential (V). From the Poisson equation and the relation between the electric field and the potential in the channel, the electric field distribution in the accumulation channel is:

$$F_x = \left[\left(\frac{2}{\varepsilon_0 \varepsilon_r}\right)\left|\int_0^V e\rho\,(V')\,\mathrm{d}V'\right|\right]^{1/2}, \tag{7}$$

where V' is the local potential, which varies from zero far away in the semiconductor bulk to V in the accumulation channel, ε_r is the relative dielectric constant of the semiconductor, and ρ is the density of charge carriers. The potential distribution if found from $x = \int_V^{V_0} \frac{\mathrm{d}V'}{F_x(V')}$, where V_0 is the surface potential at the semiconductor/insulator interface. The boundary conditions are given by: $F_x(0) = F_x(V = V_0)$,

Table 2 Parameters T_0 (the width of the exponential density of states), σ_0 (the conductivity prefactor), α^{-1} (the effective overlap parameter), $\mu_{FET}(V_g)$ (the field-effect mobility determined from Eq. (3) at $V_g = -19$ V and room temperature).

polymer	T_0 (K)	σ_0 (10^6 S/m)	α^{-1} (Å)	$\mu_{FET}(V_g)$ (m^2/Vs)
$OC_{10}C_{10}$-PPV	340	0.13	2.6	8.7×10^{-8}
OC_1C_{10}-PPV	540	31	1.4	4.7×10^{-8}
NRS-PPV	560	3.5	1.36	4.0×10^{-9}

which is the electrical field at the S/I interface and $\rho_{ind} = \varepsilon F_x(V_0)$, which is the induced charge per unit area. The gate voltage is related to ρ_{ind} as follows: $V_g = \rho_{ind}/C_i + V_{fb}$, where V_{fb} is the flat-band voltage and is neglected in these calculations. Now the distribution of the charge carrier density in the accumulation layer can be calculated as function of distance x for every gate voltage [20].

In order to model the experimental transfer characteristics obtained on the three polymer based FETs, we use the variable range hopping model developed by Vissenberg and Matters [12]. Using a percolation model of variable range hopping, the conductivity has been determined as a function of the density of charge carriers and temperature [12]. From the conductivity an expression for the local mobility as a function of charge carrier density can be derived:

$$\mu_{FET}(p) = \frac{\sigma_0}{e}\left[\frac{\left(\frac{T_0}{T}\right)^4 \sin\left(\pi\frac{T}{T_0}\right)}{(2\alpha)^3 B_c}\right]^{T_0/T} p^{\frac{T_0}{T}-1} \tag{8}$$

where σ_0 is a prefactor for the conductivity, α^{-1} is the effective overlap parameter between localised states and $B_c \cong 2.8$ is the critical number for the onset of percolation. Taking into account the distribution of the charge carrier density perpendicular to the channel the field-effect current is calculated using the integration over the accumulation channel $I_{ds} = WV_d/L \int_0^t ep(x)\,\mu(p(x))\,dx$, where t represents the thickness of the accumulation channel. Using this formalism the dc transfer characteristics of the PPV-derivatives can be modelled as a function of T and V_g. The fit parameters T_0, σ_0, α^{-1} are given in Table 2. The calculated transfer characteristics are shown in Figs. 4 and 5 as solid lines. Good agreement has been obtained for all three semiconductors [13]. It should be noted that at high gate voltages the charge carriers are strongly confined to the interface, approaching a 2-D transport system. Therefore, one could expect that the percolation threshold B_c is modified as compared to the 3-D model used by Vissenberg and Matters. However, the model based on the 3-D percolation threshold consistently describes the charge transport both a low gate bias, where the system is more 3-D like, and high gate voltages. This indicates that the effect of an eventual 3-D to 2-D change in the type of percolation will not be very large. A description about a possible gate voltage dependence of B_c is beyond the scope of this paper.

Subsequently, by combining Eq. (8), using the parameters as determined from the experimental transfer characteristics, with the distribution of the charge carrier density as a function of x, the local mobility in the accumulation channel can be calculated. In Fig. 7 the distribution of the local mobility versus distance x from the interface is presented together with the experimental field-effect mobility from Eq. (3) for OC_1C_{10}-PPV at a gate voltage $V_g = -19$ V. We find that the local mobility decreases about one order of magnitude in the first 2 nm from the semiconductor/insulator interface into the bulk. The local mobility of the charge carriers directly at the semiconductor/insulator interface is about 15% larger as compared with the experimental field-effect mobility determined from Eq. (3), which represents an average over all the induced carriers. As a consequence, the error due to the approximation in Eq. (3) that all the

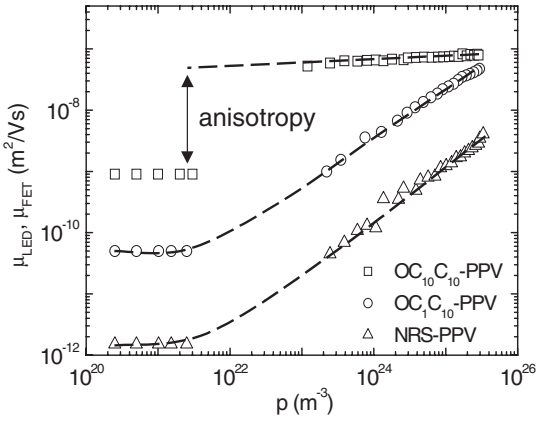

Fig. 8 Hole mobility as a function of charge carrier density in diode and field-effect transistor for NRS-PPV, OC_1C_{10}-PPVand $OC_{10}C_{10}$-PPV. The dashed line is a guide for the eye.

charge carriers in the accumulation layer have the same mobility is relatively small. The reason for this relatively small difference is that not only a major part of the charge carriers is located close to the interface, but also that these charge carriers have the highest mobility. As a result the field-effect current is mainly determined by the charge carriers directly at the interface.

2.3 Comparison of the hole mobility in LEDs and FETs

The charge carrier mobility as function of charge carrier density as obtained from the field-effect transistors at room temperature is shown in Fig. 8, together with the mobility of the hole-only diodes. At low bias voltages the SCL current of the hole-only diode is exactly quadratic, indicative of a constant mobility. Consequently, at low bias voltage the hole mobility is independent of both electric field and charge carrier density. The lowest charge carrier density p_L in a space-charge limited diode is found at the non-injecting contact and is given by:

$$p_L = \frac{3}{4}\left(\frac{\varepsilon_0 \varepsilon_r V}{eL^2}\right), \tag{9}$$

where L represents the thickness of the polymer layer. For the diode structures studied here the low bias range corresponds to hole densities of typically 2.5×10^{20} to 2.5×10^{21} m^{-3}. For high bias voltage the dependence of the mobility on the charge carrier density and on the electric field cannot be disentangled due to the fact that in a space charge limited diode both these parameters increase simultaneously. The values of the experimental field-effect mobility have been calculated using Eq. (3). Combination of the results from the diode and field-effect measurements shows that typically the hole mobility is constant for charge carrier densities $<10^{22}$ m^{-3} and increases with a power law for charge carrier densities $>10^{22}$ m^{-3}. As demonstrated in Fig. 8 the mobility differences of up to three orders of magnitude obtained from diodes and FETs, based on a single disordered polymer (OC_1C_{10}-PPV or NRS-PPV), originates from the different charge density regimes in these devices. Although it has been demonstrated that in OC_1C_{10}-PPV the optical properties exhibit a significant anisotropy [21], a possible anisotropy in the charge transport properties would obscure a direct comparison between diodes and FETs. As shown from Eq. (2) the amount of energetic disorder is directly reflected in the thermal activation of the low-field mobility. For the (logarithm of) low-field mobility obtained from PPV-based LEDs it is difficult to discriminate whether its temperature dependence scales with $1/T$ or $1/T^2$ (Eq. (2)), due to the limited temperature range accessible in the experiments (150–300 K). When plotted against $1/T$ the mobility is also well described by $\mu \sim \exp\left(-E_a/k_B T\right)$, and an activation energy E_a of typically 0.48 eV has been reported [15]. Also for transistors the field-effect mobility is thermally activated by a gate-voltage dependent activation energy [22]. In Fig. 9 the activation energy E_a of the field-effect mobility is plotted for OC_1C_{10}-PPV as a function of gate voltage from –1 to –19 V. Extrapolation towards $V_g = 0$ V yields an

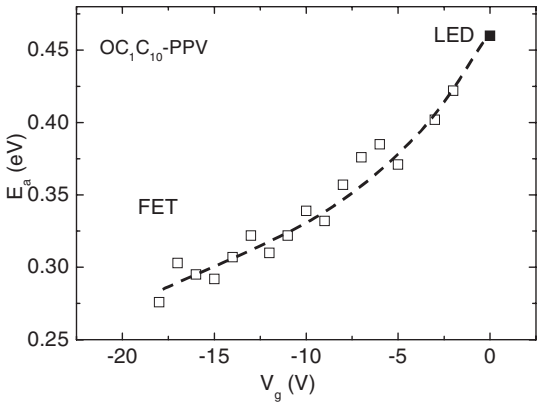

Fig. 9 Activation energy of the mobility in OC_1C_{10}-PPV diode (closed square) and FET (open squares) as a function of voltage.

E_a of 0.46 eV, exactly equal to the activation energy as obtained from the diode measurements on this polymer. This is a strong indication for the absence of anisotropy in the charge transport properties of this polymer. The absence of anisotropy has also been observed for NRS-PPV. In contrast, for $OC_{10}C_{10}$-PPV the mobility behaviour in Fig. 8 clearly shows a lack of correlation in mobility between diode and field-effect transistor measurements. The explanation is that OC_1C_{10}-PPV and NRS-PPV are highly disordered systems in which the charge transport takes place in 3-D. $OC_{10}C_{10}$-PPV is on the other hand more ordered due to the two symmetric side-chains and the charge transport is different in the directions parallel and perpendicular to the polymeric film.

In order to compare the two theoretical models used to explain the charge carrier transport in LEDs and FETs, we plotted the Gaussian DOS (Eq. (1)) and the exponential DOS (Eq. (4)) as function of energy for our devices. In Fig. 10 and 11 the Gaussian DOS, as obtained from the temperature dependent diode measurements, is plotted as a function of energy for NRS-PPV and OC_1C_{10}-PPV, respectively. For the total number of states per unit volume N_t we have used a value of 3×10^{26} m^{-3} for both OC_1C_{10}-PPV and NRS-PPV. Additionally, the exponential DOS, described by T_0 (See Table 2), of OC_1C_{10}-PPV and NRS-PPV as obtained from the FET characteristics are shown. With increasing gate voltage up to –19 V the Fermi-level in the Gaussian DOS ranges from 0.4 eV to 0.16 eV with respect to the centre of the Gaussian DOS for the OC_1C_{10}-PPV based FET, and from 0.42 eV to 0.17 eV for the NRS-PPV based FET. From Figs. 10 and 11 we find that in this energy range the exponential distribution is a good approximation of the Gaussian DOS. In this way the two models are unified, in the sense that the exponential DOS accurately describes the Gaussian DOS in the energy range in which the field-effect transistors operate. Consequently, the temperature- and charge carrier density dependencies of the hole mobility in

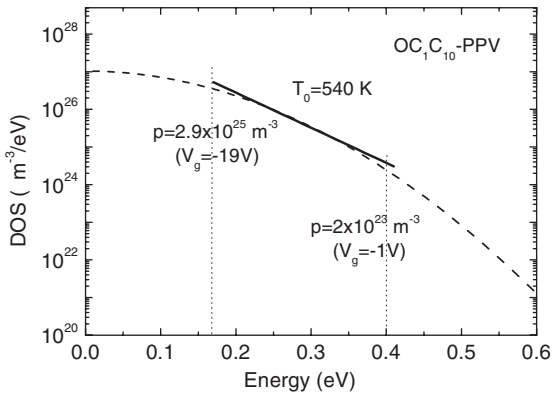

Fig. 10 Gaussian density of states (DOS) (dashed line) and the exponential DOS (solid line) as a function of energy for OC_1C_{10}-PPV.

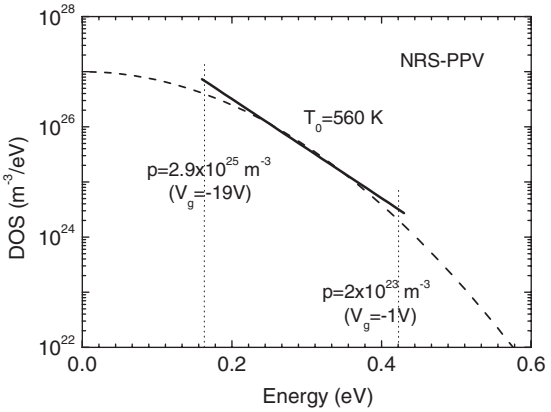

Fig. 11 Gaussian density of states (DOS) (dashed line) and the exponential DOS (solid line) as a function of energy for NRS-PPV.

these disordered conjugated polymers are unified in one single charge transport model. An effect that we ignored in this comparison is that the density of states could be modified due to the induced charges. Recent model caculations demonstrated that an increase of the doping level also increases the energetic disorder due to potential fluctuations caused by the Coulomb field of randomly distributed dopant ions [23]. In a FET the charge carrier density is increased by a gate field. The fact that the models for LED and FET can be unified indicates that the effect of the induced charge alone, without ions, is less pronounced in the used gate voltage range.

3 Conclusions

In conclusion, we investigated the hole mobility for three PPV derivatives in hole-only diodes and field-effect transistors as function of bias and temperature. It has been show that the experimental hole mobility for a single polymer based diode and FET can differ by 3 orders of magnitude. This discrepancy originates from the strong dependence of the hole mobility on the charge carrier density. For highly disordered PPVs it is demonstrated that the exponential density of states (DOS), which theoretically describes the charge transport in FETs, is a good approximation of the tail states of the Gaussian DOS, which describes the charge transport in LEDs. Increase of the directional order in the polymeric PPV film leads to an increase of the hole mobility in both diodes and FETs, but also to a strong anisotropy in the charge transport between the two types of devices.

Acknowledgements This work is part of the research programme of the Dutch Polymer Institute.

References

[1] J. H. Burroughes, D. D. C. Bradley, A. R. Brown, R. N. Marks, K. Mackay, R. H. Friend, P. L. Burn, and A. B. Holmes, Nature (London) **347**, 539 (1990).
[2] P. W. M. Blom, M. C. J. M. Vissenberg, J. N. Huiberts, H. C. F. Martens, and H. F. M. Schoo, Appl. Phys. Lett. **77**, 2057 (2000).
[3] H. Sirringhaus, N. Tessler, and R. H. Friend, Science **280**, 1741 (1998).
[4] H. E. A. Huitema, G. H. Gelinck, J. B. P. H. van der Putten, K. E. Kuijk, C. M. Hart, E. Cantatore, P. T. Herwig, A. J. J. M. van Breemen, and D. M. de Leeuw, Nature **414**, 599 (2001).
[5] H. Bässler, phys. status solidi (b) **175**, 15 (1993).
[6] S. V. Novikov, D. H. Dunlap, V. M. Kenkre, P. E. Parris, and A. V. Vannikov, Phys. Rev. Lett. **81**, 4472 (1998).
[7] H. Sirringhaus, P. J. Brown, R. H. Friend, M. M. Nielsen, K. Bechgaard, B. M. W. Langeveld-Voss, A. J. H. Spiering, R. A. J. Janssen, E. W. Meijer, P. T. Herwig, and D. M. de Leeuw, Nature (London) **401**, 685 (1999).
[8] S. F. Nelson, Y.-Y. Lin, D. J. Gundlach, and T. N. Jackson, Appl. Phys. Lett. **77**, 1854 (1998).
[9] R. H. Friend, Y.-Y. Lin, R. W. Gymer, A. B. Holmes, J. H. Burroughes, R. N. Marks, C. Taliani, D. D. C. Bradley, D. A. Dos Santos, J. L. Brédas, M. Lögdlung, and W. R. Salaneck, Nature (London) **397**, 121 (1999).
[10] C. D. Dimitrakopoulos and P. R. L. Malenfant, Adv. Mater. **14**, 99 (2002).
[11] G. H Gelinck, H. E. Huitema, E. van Veenendaal, E. Cantatore, L. Schrijnemakers, J. B. P. H. van der Putten, T. C. T. Geuns, M. Beenhakkers, J. B. Giesbers, B.-H. Huisman, E. J. Meijer, E. Mena Benito, F. J. Touwslager, A. W. Marsman, B. J. E. van Rens, and D. M. de Leeuw, Nature Mater. **3**, 106 (2004).
[12] M. C. J. M. Vissenberg and M. Matters, Phys. Rev. B **57**, 12964 (1998).
[13] C. Tanase, E. J. Meijer, P. W. M. Blom, and D. M. de Leeuw, Phys. Rev. Lett. **91**, 216601 (2003).
[14] Y. Roichman and N. Tessler, Appl. Phys. Lett. **80**, 1948 (2002).
[15] P. W. M. Blom and M. C. J. M. Vissenberg, Mater. Sci. Eng. **27**, 53 (2000).
[16] H. C. F. Martens, P. W. M. Blom, and H. F. M. Schoo, Phys. Rev. B **61**, 7489 (2000).
[17] M. Kemerink, J. K. J. van Duren, P. Jonkheijm, W. F. Pasveer, P. M. Koenraad, R. A. J. Janssen, H. W. M. Salemink, and J. H. Wolter, Nano Lett. **3**, 1191 (2003).
[18] A. R. Brown, C. P. Jarrett, D. M. de Leeuw, and M. Matters, Synt. Met. **88**, 37 (1997).
[19] S. M. Sze, Physics of Semiconductor Devices (Wiley, New York, 1981).
[20] C. Tanase, E. J. Meijer, P. W. M. Blom, and D. M. de Leeuw, Org. Electron. **4**, 33 (2003).
[21] C. M. Ramsdale and N. C. Greenham, Adv. Mater. **14**, 212 (2002).
[22] E. J. Meijer, M. Matters, P. T. Herwig, D. M. de Leeuw, and T. M. Klapwijk, Appl. Phys. Lett. **76**, 3433 (2000).
[23] V. I. Arkhipov, P. Heremans, E. V. Emelianova, G. J. Adriaensses, and H. Bässler, Appl. Phys. Lett. **82**, 3245 (2003).